

Laser-assisted thermal imprinting of glass guided mode resonant (GMR) optical filter

Helen Lee May Shian, Syarifah Nur Hasanah Binti Syed Kamarudin, Ismayuzri Bin Ishak, Ahmad Shahir Jamaludin, Ahmad Rosli Abdul Manaf and Mohd Zairulnizam Bin Mohd Zawawi*

Faculty of Manufacturing and Mechatronics Engineering Technology, Universiti Malaysia Pahang, 26600, Pekan, Pahang, Malaysia

ABSTRACT – Thermal imprinting is a promising low cost and reliable method for direct replication of glass nanostructures without the use of mask and the serial lithography and etching processes. However, direct thermal imprinting on glass is a very challenging task and it is difficult to obtain complete replication height even with long pressing time and high pressing load. In this paper, laser-assisted thermal imprinting of glass nanostructures was demonstrated. Compare to the conventional glass thermal imprinting, this method significantly reduced the contact imprinting time and imprinting load while preserving the replication fidelity. The quality of the replicated glass nanostructures revealed by field emission scanning electron microscope (SEM) and atomic force microscope (AFM) exhibited a very smooth surface finish that closely matched the profile of the silicon mold. As proof-of-concept, the utility of laser-assisted, imprinted glass nanostructures as guided mode resonant (GMR) optical filter was evaluated. The peak spectral values obtained were satisfactory; which yielded an average full width at half maximum (FWHM) and peak wavelength value (PWV) of 4.6 nm and 691.39 nm respectively. This method provide a new alternative for a more energy efficient and rapid fabrication of nanostructured glass optical devices.

ARTICLE HISTORY

Revised: 30th March 2021

Accepted: 31st March 2021

KEYWORDS

Laser-assisted, guided mode resonants (GMR), optical filter, thermal imprinting, optical glass

INTRODUCTION

Nanostructured surface can provide numerous advanced and useful function such as for biosensors[1-3], imaging[4-6], point-of-care testing (POCT) for medical diagnostics[7-9] and biomimetics[10-12]. Glass-based micro/nano structured devices are more desirable, since there are superior in terms of imaging performance, thermal stability and chemical resistance compare to its polymer counterpart. To reduce the process cycle time as well as the manufacturing cost, new fabrication techniques to obtain nanostructured glass surfaces have been an interesting research topic recently.

At present, the fabrication of nanostructured glass devices relies on the well-established semiconductor manufacturing techniques, for example photolithography[13], extreme ultraviolet lithography (EUV)[14], electron beam lithography (EBL) and etching[15]. These fabrication processes are well known to be very accurate and reliable. Nevertheless, these processes require very expensive and sophisticated equipment, low in throughput and not suitable for mass production. In addition, all the process must be carried out in a clean room environment. Direct laser texturing had also been demonstrated. Nevertheless, the process of writing the small pattern features size such as nanograting, nanoholes or nanopillars is time consuming. Besides that, secondary process such as etching and heat treatment is necessary to improve the morphology and surface roughness of the pattern. Mechanical machining on glass had also been demonstrated. Unfortunately, the pattern resolution that can be achieved typically could not be less than 50 μm [16-17]. High surface roughness value of the machined glass surface also generally cannot be used in the application of high precision optical devices. In the meantime, thermal imprinting also had been identified as one of a promising method due to its relatively low-cost equipment setup[18-21]. However, several problems are recognized in the existing conventional glass thermal imprinting including a long thermal cycle and difficulties in ensuring good imprinting quality.

In this paper, a rapid energy-efficient method to directly pattern nanoscale features on glass substrate using thermal imprinting combined with CO₂ laser irradiation was proposed. Prominently, this method utilizes a CO₂ which irradiates through an infrared (IR) transparent mold. The glass strongly absorbed the 10.6 μm wavelength irradiation for CO₂ laser triggering substantial heating of a thin layer on the glass surface, which significantly enhanced the filling of pressed glass

material into nanostructured mold cavities. As proof-of-concept of our work, we evaluated the utility of laser-assisted, imprinted glass nanostructures as GMR sensors.

EXPERIMENTAL SETUP

Figure 1 shows the schematic of the custom built laser assisted thermal imprinting system which consists of a CO₂ laser head, a reflective mirror, a beam expander and a mold assembly. The mold assembly includes top plate, upper insulator and upper heating block with a drilled hole opening at the center of the for the laser beam to pass through, lower heating block, lower insulator and cartridge heaters. Both the upper and lower heating block were made of heat treated hot work tool steels, grounded to mirror surface finish and coated with 1 μ m diamond like carbon (DLC). The silicon mold with nanograting structures was attached circumferentially at the upper heating block by means of mechanical clamping. Two sheathed K-type thermocouples were embedded at the center of the molds connected to PID controller and data logger for online monitoring of the mold temperature profile. An external computer controlled program was used to set the desired laser beam intensity profile. CO₂ laser which can deliver a maximum power of 30W and the operating wavelength is 10.6 μ m was used. The procedure of the imprinting begins by first applying a pressure to the glass sandwiched between the silicon mold and the flat lower mold. Then immediately the laser irradiation with laser beam diameter of 3mm at $1/e^2$ from the laser source was enlarged accordingly by laser beam expander propagates through the transparent silicon mold and absorbed by the glass. To avoid glass fracture due to the sudden temperature rise induced from the laser source, the bulk of the glass was preheated. After the laser irradiation was interrupted, the upper mold was retracted and glass was released for cooling.

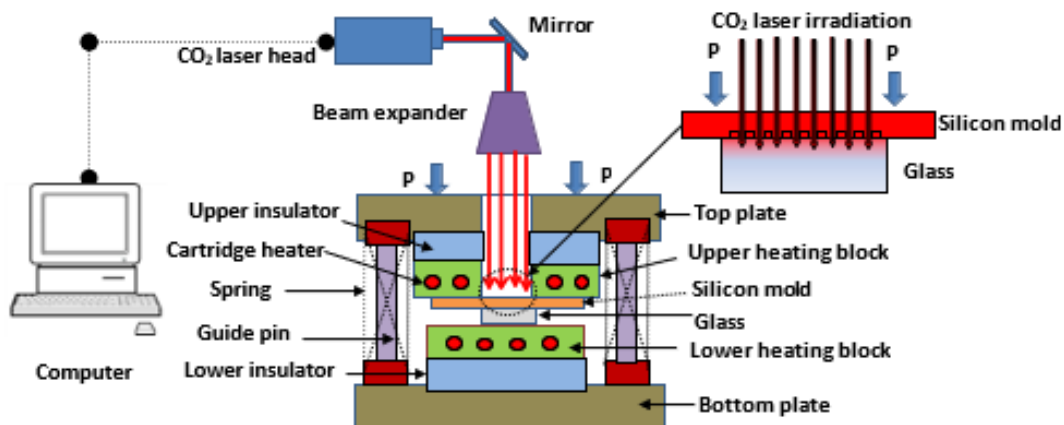


Figure 1: Schematic diagram of the CO₂ laser assisted thermal imprinting setup

RESULT AND DISCUSSION

Imprinted Pattern Quality

The replication quality of the laser-assisted imprinted glass was characterized using SEM and AFM measurement. The SEM images and AFM morphologies of the silicon molds and imprinted glasses are shown in Figure 2 and Figure 3 respectively. Glass was imprinted via one-spot laser irradiation (power 30 W, laser irradiation time 5 s, beam diameter 2.5 mm, imprinting load 0.4 MPa). Based on many trials, under above conditions, laser irradiation time for about 5 s ensured replication pattern fidelity. The replication width and height very closely matched the inverse values of the silicon mold. However, when assessing imprint height, measurement error was possible; the thickness and location of the measurement line defined by the operator might be associated with errors ± 20 nm. The discrepancies were very small; the flat rectangular profile of the polished crosssectional SEM image showed that the replication height was as expected [Figure 2(b)]. We believed that the successful rapid imprinting indicates that our proposed fabrication method was minimally dependent on feature size when using laser assisted imprinting. To achieve complete pattern transfer employing conventional glass thermal imprinting, optimization of temperature, pressure, and holding time are highly dependent on pattern size (thus the line width, and the duty and aspect ratios). It should be noted that the total cycle time for thermal imprinting previously demonstrated in the literature are generally more than 15 minutes [18,21,22]. The data imply that the method could be used to imprint even smaller nanoscale patterns of higher aspect ratio; this is a task for the future.

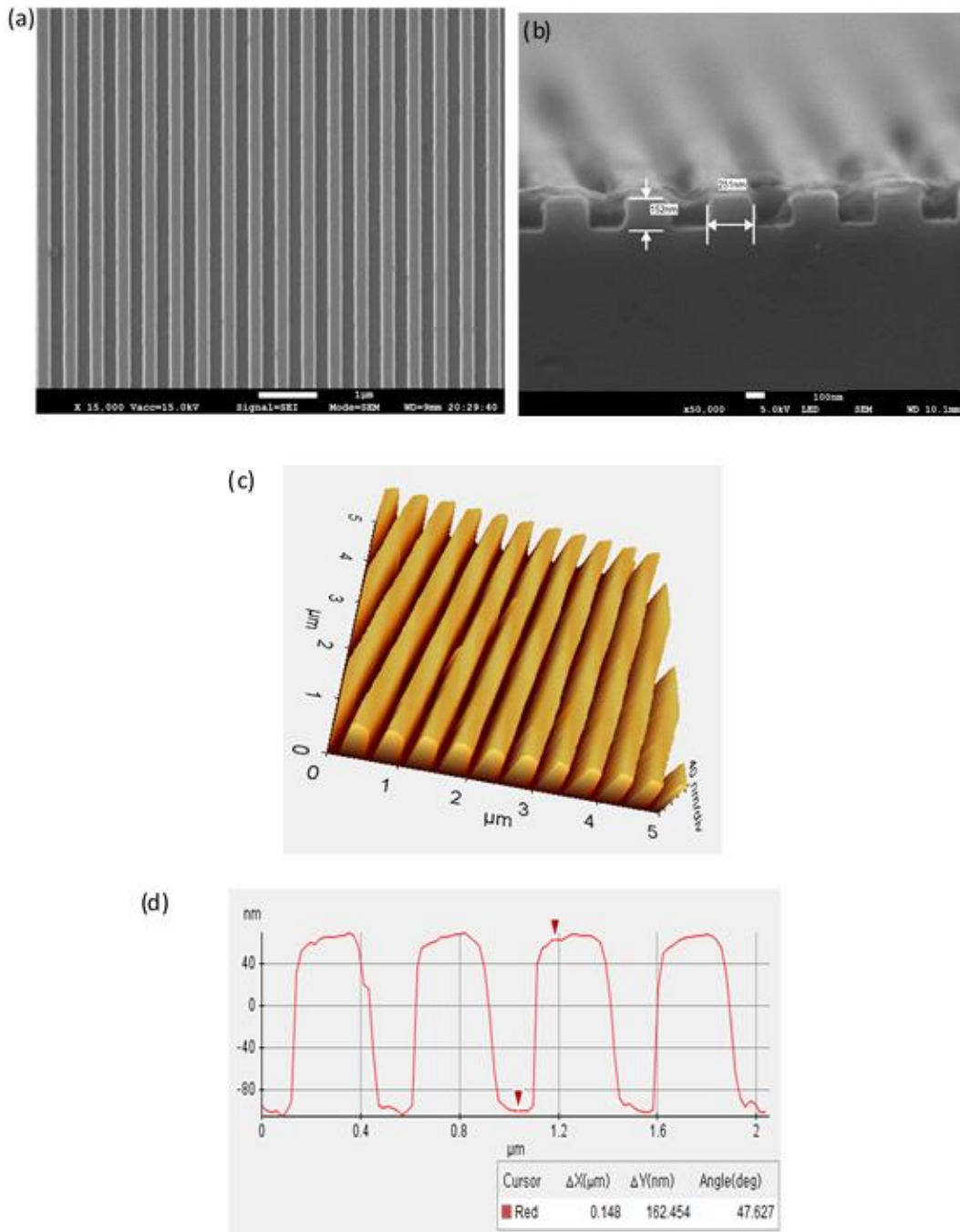


Figure 2: (a) SEM image (top view), b) SEM image of the polished cross section, c) an AFM 3D profile and d) an AFM 2D cross-section of the silicon mold. The nanograting pattern was 230 nm line width, 455 nm pitch and 155 nm height.

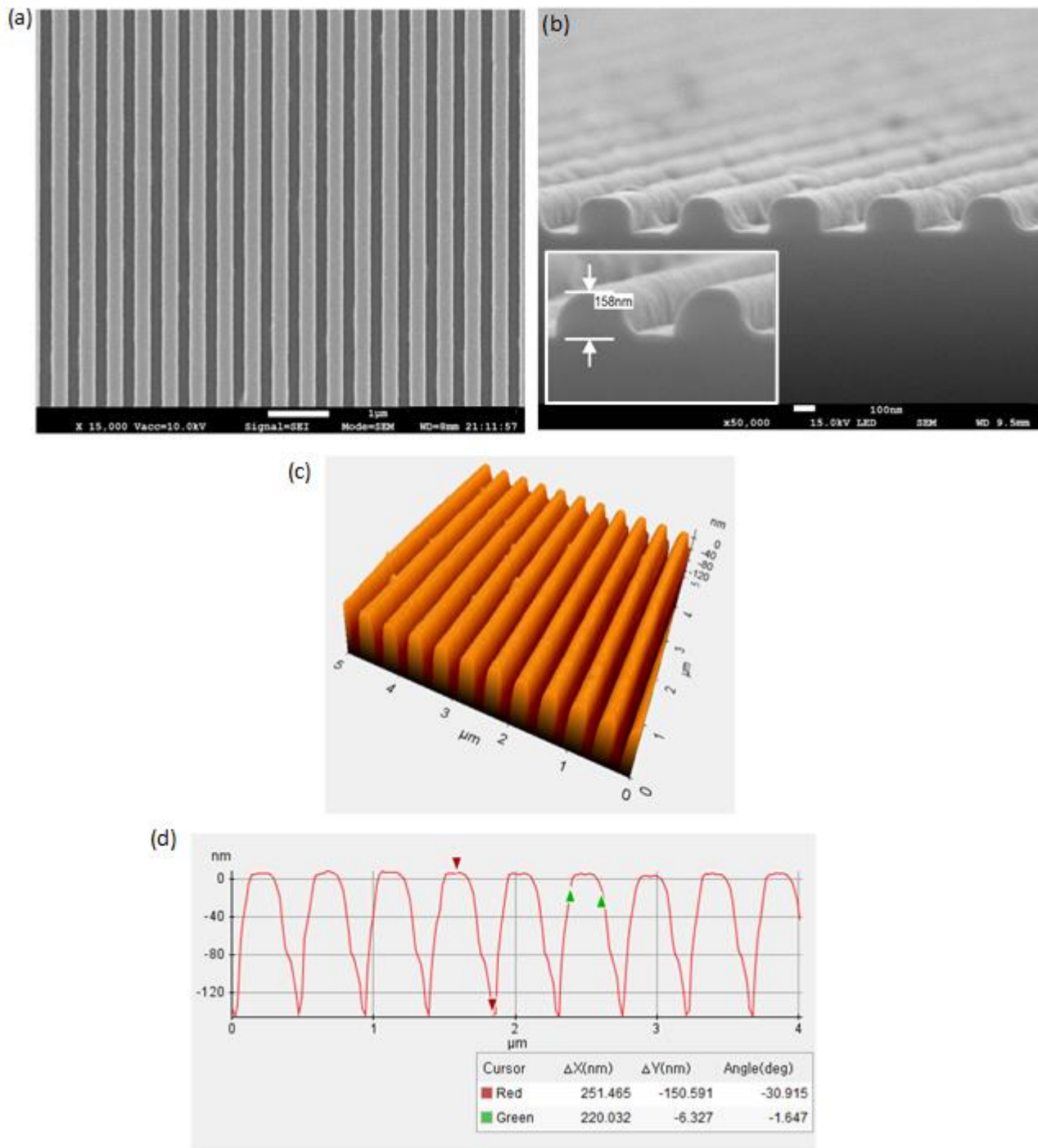


Figure 3: (a) SEM image (top view), b) SEM image of the polished cross section; inset view showing an enlarge view, c) an AFM 3D profile and d) an AFM 2D cross-section, of the imprinted glass obtained via the CO₂ laser-assisted scanning process. The imprinted nanograting pattern was 230 nm line width, 460 nm pitch and 155 nm height.

Evaluation of Laser-assisted Thermal Imprinting of a Guided Mode Resonant Optical Filter

To evaluate the performance of a laser-assisted, imprinted guided mode resonant (GMR) optical filter, a glass surface with a nanograting was coated with 115 nm of silicon nitride Si_3N_x of refractive index 2.05 via plasma-enhanced chemical vapor deposition (PECVD). From top to bottom, the device featured an air layer, Si_3N_4 , and the substrate glass. The method used to evaluate filter performance [using an Ocean Optics spectrometer and transverse magnetic (TM) polarized white light] is shown in Figure 4. Based on the measurement, the full width at half maximum (FWHM) and peak wavelength value (PWV) were recorded.

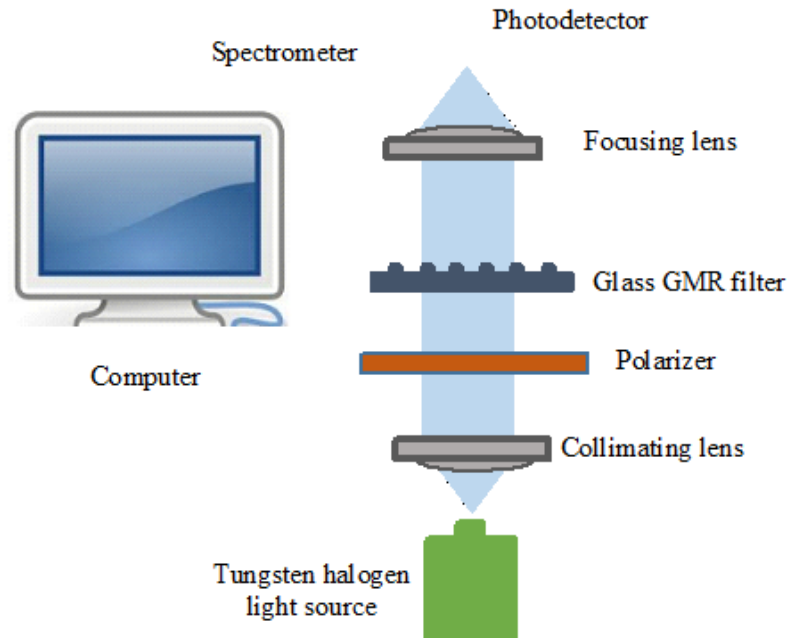


Figure 4: Measurement of FWHM, PWV and PWV shift using white light source and spectrometer system Schematic

Six samples were evaluated three times, and averages calculated. Figure 5 shows the FWHM and PWV data collected after addition of phosphate-buffered saline (PBS) to the tops of the samples. The average FWHM and PWV were 4.6 and 691.39 nm respectively (Table 1). Rigorous coupled wave analysis (RCWA) simulation yielded FWHM and PWV values of about 0.5 and 690 nm respectively. The differences may be attributable to any one of several factors. The simulation assumed that the nanograting was perfectly rectangular and smooth-walled. However, fabrication errors such as reductions in grating width and height caused by shrinkage, variations in the thickness of the silicon nitride coating and the roughness of the nanograting surface and wall are to be expected. Notably, GMR filters are very sensitive to fabrication error. Here, the nanograting design was not optimized prior to simulation, but the peak spectral values were satisfactory and the device sensitive. Although not demonstrated in this study, it is fair to assume that the glass GMR optical filter will exhibit better temperature stability than filters fabricated from polymers, which generally degrade above 100°C.

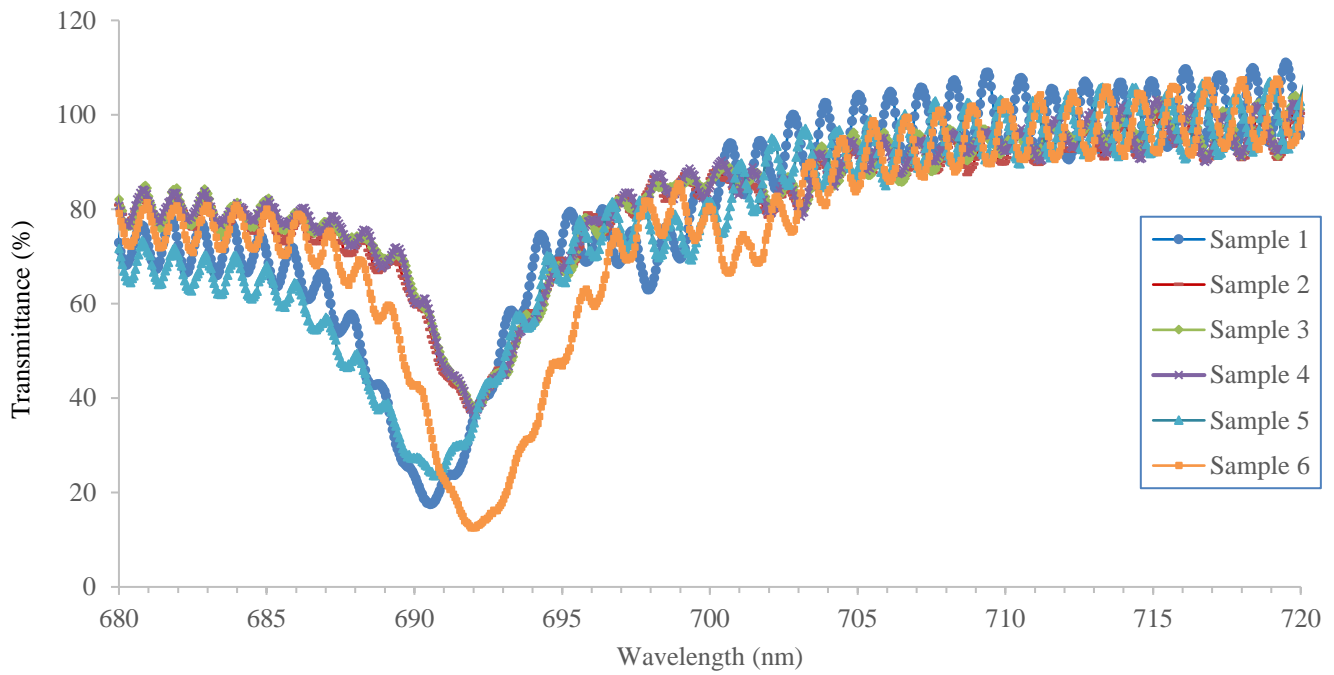


Figure 5: PWV and FWHM measurement of the laser assisted imprinted glass GMR filter via spectrometer

Table 1: Measured FWHM and PWV value of the glass GMR optical filter obtained via the spectrometer

Sample No.	Measured FWHM (nm)	Measured PWV (nm)
1	4.5	690.53
2	4.5	692.02
3	4	691.91
4	4	692.08
5	6	691.14
6	5	690.64
Average	4.6	691.39

CONCLUSION

We imprinted a high-quality nanograting onto K-PG375 optical glass using laser-assisted thermal imprinting. The pattern exhibited a very smooth surface finish that closely matched the profile of the silicon mold. The nanograting (LS 230 nm; height 160 nm) was deposited onto 100-nm-thick highly refractive SiN_x and integrated with a spectrometer, wherein the nanograting served as a GMR optical filter. The average FWHM and PWV were 4.6 and 691.39 nm respectively. Even though the nanograting design was not optimized prior to simulation, but the peak spectral values were satisfactory and the device sensitive. The detail evaluation performance of fabricated glass as a GMR label-free biosensor is ongoing.

ACKNOWLEDGEMENT

This research was partially supported by Fundamental Research Grant Scheme, FRGS/1/2019/TK03/UMP/03/8 with the grant number RDU1901216, Ministry of Higher Education, Malaysia (MOHE).

REFERENCES

- [1] Fannin, Alexander L., Brett R. Wenner, Jeffery W. Allen, Monica S. Allen, and Robert Magnusson. "Properties of mixed metal–dielectric nanogratings for application in resonant absorption, sensing, and display." *Optical Engineering* 56, no. 12 (2017): 121905.
- [2] Palinski, Timothy J., Brian E. Vyhnalek, Gary W. Hunter, Amogha Tadimety, and John XJ Zhang. "Mode Switching With Waveguide-Coupled Plasmonic Nanogratings." *IEEE Journal of Selected Topics in Quantum Electronics* 27, no. 1 (2020): 1-10.
- [3] Yamada, Katsuki, Kyu Jin Lee, Yeong Hwan Ko, Junichi Inoue, Kenji Kintaka, Shogo Ura, and Robert Magnusson. "Flat-top narrowband filters enabled by guided-mode resonance in two-level waveguides." *Optics letters* 42, no. 20 (2017): 4127-4130.
- [4] Zhang, Yang, Ge Wang, Lu Yang, Fei Wang, and Aihua Liu. "Recent advances in gold nanostructures based biosensing and bioimaging." *Coordination Chemistry Reviews* 370 (2018): 1-21.
- [5] Liu, Yanhuan, Weiliang Guo, and Bin Su. "Recent advances in electrochemiluminescence imaging analysis based on nanomaterials and micro-/nanostructures." *Chinese Chemical Letters* 30, no. 9 (2019): 1593-1599.
- [6] Xu, Canhua, Jing Ma, Chaozhen Ke, Yantang Huang, Zhiping Zeng, Weixiang Weng, Lituo Shen, and Kangjun Wang. "Full-Stokes polarization imaging based on liquid crystal variable retarders and metallic nanograting arrays." *Journal of Physics D: Applied Physics* 53, no. 1 (2019): 015112.
- [7] Ke, Yonggang, Carlos Castro, and Jong Hyun Choi. "Structural DNA nanotechnology: artificial nanostructures for biomedical research." *Annual review of biomedical engineering* 20 (2018): 375-401.
- [8] Park, Jeong-Eun, Minho Kim, Jae-Ho Hwang, and Jwa-Min Nam. "Golden opportunities: Plasmonic gold nanostructures for biomedical applications based on the second near-infrared window." (2017): 1600032.
- [9] Jafari, Sevda, Baharak Mahyad, Hadi Hashemzadeh, Sajjad Janfaza, Tooba Gholikhani, and Lobat Tayebi. "Biomedical applications of tio2 nanostructures: recent advances." *International Journal of Nanomedicine* 15 (2020): 3447.
- [10] Wen, Gang, ZhiGuang Guo, and Weimin Liu. "Biomimetic polymeric superhydrophobic surfaces and nanostructures: from fabrication to applications." *Nanoscale* 9, no. 10 (2017): 3338-3366.
- [11] Son, Taeho, Eunjin Yang, Eusun Yu, Kyu Hwan Oh, Myoung-Woon Moon, and Ho-Young Kim. "Effects of surface nanostructures on self-cleaning and anti-fogging characteristics of transparent glass." *Journal of Mechanical Science and Technology* 31, no. 11 (2017): 5407-5414.
- [12] Haghanifar, Sajad, Ping Lu, Md Imrul Kayes, Susheng Tan, Ki-Joong Kim, Tongchuan Gao, Paul Ohodnicki, and Paul W. Leu. "Self-cleaning, high transmission, near unity haze OTS/silica nanostructured glass." *Journal of Materials Chemistry C* 6, no. 34 (2018): 9191-9199.
- [13] Bae, Sang-In, Kisoo Kim, Sungpyo Yang, Kyung-won Jang, and Ki-Hun Jeong. "Multifocal microlens arrays using multilayer photolithography." *Optics express* 28, no. 7 (2020): 9082-9088.

- [14] Peng, Xiaoman, Yafei Wang, Jian Xu, Hua Yuan, Liangqian Wang, Tao Zhang, Xudong Guo, Shuangqing Wang, Yi Li, and Guoqiang Yang. "Molecular Glass Photoresists with High Resolution, Low LER, and High Sensitivity for EUV Lithography." *Macromolecular Materials and Engineering* 303, no. 6 (2018): 1700654.
- [15] Kanamori, Yoshiaki, Hisao Kikuta, and Kazuhiro Hane. "Broadband antireflection gratings for glass substrates fabricated by fast atom beam etching." *Japanese Journal of Applied Physics* 39, no. 7B (2000): L735.
- [16] Mishra, Dileep Kumar, Julfekar Arab, Karan Pawar, and Pradeep Dixit. "Fabrication of deep microfeatures in glass substrate using electrochemical discharge machining for biomedical and microfluidic applications." In *2019 IEEE 21st Electronics Packaging Technology Conference (EPTC)*, pp. 263-266. IEEE, 2019.
- [17] Ikwuagwu, Ikwuagwu, Amirkianoosh Kiani, and Jana D. Abou Ziki. "Hybrid method combining SACE micro-machining and laser processing to fabricate glass micro-features with special surface properties." *IFAC-PapersOnLine* 52, no. 10 (2019): 311-314.
- [18] Jang, Hyungjun, Muhammad Refatul Haq, Youngkyu Kim, Jun Kim, Pyoung-hwa Oh, Jonghyun Ju, Seok-Min Kim, and Jiseok Lim. "Fabrication of glass microchannel via glass imprinting using a vitreous carbon stamp for flow focusing droplet generator." *Sensors* 18, no. 1 (2018): 83.
- [19] Jiang, Kai, Kangsen Li, Gang Xu, Feng Gong, Xiaoyu Wu, Dongfeng Diao, and Likuan Zhu. "A novel and flexible processing for hot embossing of glass microfluidic channels." *Ceramics International* 47, no. 1 (2021): 1447-1455.
- [20] Hu, Manfeng, Jin Xie, Wei Li, and Yuanhang Niu. "Theoretical and Experimental Study on Hot-Embossing of Glass-Microprism Array without Online Cooling Process." *Micromachines* 11, no. 11 (2020): 984.
- [21] Li, Kangsen, Xinfang Huang, Qiang Chen, Gang Xu, Zhiwen Xie, Yuanyuan Wan, and Feng Gong. "Flexible fabrication of optical glass micro-lens array by using contactless hot embossing process." *Journal of Manufacturing Processes* 57 (2020): 469-476.
- [22] Ostrovsky, Natali, Dor Yehuda, Sivan Tzadka, Evyatar Kassis, Shay Joseph, and Mark Schwartzman. "Direct Imprint of Optical Functionalities on Free-Form Chalcogenide Glasses." *Advanced Optical Materials* 7, no. 19 (2019): 1900652.